Non-destructive Plant Analysis with Computer Vision and Robotics

Gerry Chen, Frank Dellaert, Yongsheng Chen

Approvals: ____________, ______________

I. Introduction

As environmental conservation is becoming an increasingly important issue, efficient agricultural practices which maximize output while minimizing resource input and environmental impact are imperative to exercise and further develop. For example, according to the EPA, nitrogen fertilizer alone contributes, in the form of N2O, at least 4.1% of total US greenhouse gas emissions [1]. Furthermore, runoff from agricultural practices causes other environmental harm such as algae blooms. Meanwhile, most common current farming practices encourage excess, blanket applications of fertilizer as opposed to the targeted, “smart” applications as part of the growing precision agriculture movement being made possible by recent advances in sensors, data, and AI [2].

Plant growth models are imperative for precision agriculture to predict crop yields under various conditions. In controls terms, the biological plant is the plant of a system, whose dynamics we must model in order to apply optimal control. Therefore, farmers seek larger amounts of real-time, actionable data on their crops while researchers seek larger amounts of higher quality, more comprehensive, more statistically significant data on plant growth to study growth models. Clearly, analysis of plants for their masses, nutrient contents, and other properties is of great interest to both farmers and researchers.

Standard methods for analyzing plant mass and nutrient content are destructive: they require harvesting the plant to weight it, dehydrate it, and send it to a lab for testing. This is not only expensive, but also significantly limits the quantity and statistical significance of data collected. For example, studying plant growth often requires tracking plant metrics as it grows, but destructive analyses make it impossible to measure the same plant multiple times since the first measurement requires killing the plant. Instead, many sets of plants must be grown under identical conditions and periodically harvested for analysis. Robotics and computer vision have been shown to offer significant value by enabling non-destructive methods for analyzing plant properties.

In this work, we propose a novel robotic system for collecting photographic data for non-destructively estimating plant properties and use the robot to collect a dataset of 56 plants. Our robot, depicted in Fig. 1 consists of a robot arm mounted on the moving platform of a cable-driven parallel robot (CDPR) to enable taking photos from a large number of viewpoints across a large number of plants. To evaluate our robot system, we collect a dataset of RGB photos of Buttercrunch Lettuce plants and their corresponding harvest masses (dry and wet). For each plant, we collect roughly 150 photos from various angles. We collect data from 56 plants, harvesting at least 9 plants at a time, 5 times in 1-week intervals to obtain data from different points in the plant growth cycle.

Fig. 1. Cable robot taking photo of plants in a hydroponic grow rig.

II. Prior Work

A. 3D Reconstruction

The works in this section analyze the 3D structures of plants using 3D reconstructions. It is useful to note that they focus on analyzing leaf area analysis, but show results only on plants with limited leaf overlap (unlike the late-stage lettuce we seek to analyze).

1) RGB: Almost all 3D reconstruction methods (even those discussed later that also use additional sensors) leverage RGB cameras given their ubiquity, low cost, and richness of information afforded by the high resolution. This section will focus on methods which use RGB cameras solely.

[3]–[5] use a single high-resolution SLR camera to manually take photographs and use photogrammetry methods to create full 3D reconstructions. The reconstructions can be computed and analyzed for leaf geometry analysis in 20-30 minutes. [6] applies a very similar method but using a handheld stereo camera rig rather than monocular.

[7] also uses stereo cameras, but also investigates leveraging salient outer-contour features in addition to traditional (sparse) 3D reconstructions.

[8], [9] both focus on estimating large-scale crop field biomass (not focusing on single-plant measurements), with [8] using UAV imagery and [9] using fixed monitoring stations with cameras.

2) Direct Depth Cameras:

a) Kinect: [10]–[12] use Kinect cameras for their ubiquity and ease of acquiring depth information, but both [10], [11] take only top-down images of the plants while [12] produces full 3D reconstructions. Since [11] focuses on analyzing leaf canopy structure, they have the distinction of analyzing high-overlap leaves (from top-down viewpoint). [12] was distinct in measuring trees instead of crop vegetable plants, but still the trees were sufficiently young (max 1 year old) that they did not exhibit much leaf overlap. [12] also estimated biomass, which is more similar to our objective than the more commonly estimated geometrical dimensions from other studies.

b) ToF cameras: Time of flight (ToF) cameras appear to be popular for their richness of information and relative compactness. [13]–[15] all use ToF cameras in combination with one or more RGB cameras to measure leaf size properties. Combining ToF with RGB leverages both the (low resolution) depth information from ToF and the high resolution color information from RGB. They are limited to indoor or greenhouse demonstrations. [13] also mounts the cameras on a robot arm. [14], [15] emphasize high-throughput phenotyping and combines RGB and ToF with high-powered flash lighting mounted on a rolling cart. High-throughput is sacrificed for fewer and less controlled plant viewpoints. Finally, while [13] applies leaf segmentation in image space before doing a 3D reconstruction, [14] applies a 3D construction first then applies leaf segmentation. [15] doesn't explicitly create a full 3D reconstruction, but segments and reasons about 3D plant properties using image-space depth maps of foreground leaves.

c) Light field (Plenoptic): Although less common, light field cameras have been used [16] as alternatives to ToF or stereo depth cameras for their improved resolution and lack of "unknown distance" pixels due to occlusion (respectively). Light field cameras operate by using special lensing techniques to capture the same image at different depths of field, which can then be analyzed to interpret scene depth information at high resolution from a single viewpoint. Due to their relative rarity, these cameras tend to be expensive despite using parts from standard 2D RGB cameras.

3) Structured Light: In [17], large numbers of fixed stereo cameras are combined with structured light to reconstruct a plant on a turntable. The reconstruction is also used to estimate plant height, number of leaves, leaf height, and inter-node distances. The work builds on previous stereo-based imaging by adding structured light to obtain better results.

The cameras are mounted on a room-scale, stationary rigid arc-shaped frame consisting of 5 stereo pairs (10 cameras total). A single random-dot pattern projector is used for the structured light, and the plant is placed on a turntable.

Their approach is to first create a point cloud by merging/registering stereo point clouds, then segment leaves. Although their headline figure would suggest that they measure large plants, the largest recorded plant in their results is less than 11 inches tall and the greatest number of leaves in one of their plants is 8. They measure on 8 cabbage, 8 cucumber, and 3 tomato plants, with all of them being young (seedling stage). They achieved accuracies roughly on the order of 5-10mm, but achieved typically correct leaf segmentations. They purport that structured light allows for fewer "glitches" in the 3D reconstructions.

B. Non-3D reconstruction

A number of methods also exist for visually estimating plant properties without 3D reconstruction.

1) Segmentation: Various techniques for 2D image processing to estimate plant properties have been used. [18]–[20] apply standard image thresholding techniques to estimate plant biomass and height/width respectively, but [19] is notable for their emphasis on high-throughput phenotyping, using a conveyor belt to rapidly photograph plants from top-down and profile views in the visible, NIR, and ultra-violet (UV) spectrums. While [19] also deals with the additional challenge of plant scaffolding (structures to support the plant as it grows) being present in the photographs requiring additional effort to remove in software using thresholding and morphology.

Crop cover area is a measure of the vertically projective area covered by leaves (≤ 1) and is measured by a number of surprisingly sophistocated techniques [21]–[27] including with deep learning [28], [29].

2) Leaf Area Index: Leaf area index is a measure which describes the ratio of leaf area to ground area (can be > 1 in case of leaf overlap). It can be straightforwardly estimated e.g. using upward facing cameras to look up at a tree canopy, however this is an only a crude estimate and leverages statistical assumptions or direct measurement calibrations regarding leaf coverage as a function of sky gap [30]–[34]. Some more advanced methods have been developed e.g. using color spectra to better estimate overlap [35].

III. Approach: Robot Design

The robot used for collecting photographic data of the lettuce plants consists of 2 subsystems: a robot arm mounted on the end effector of a cable-driven parallel robot (CDPR). The purpose of the robot arm is to collect large numbers

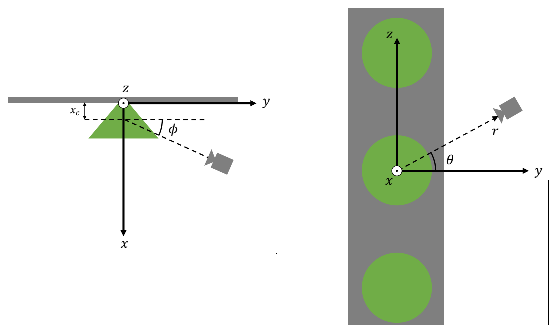

(a) Top view (b) Front view

Fig. 2. Coordinate frame of the camera with respect to a lettuce plant.

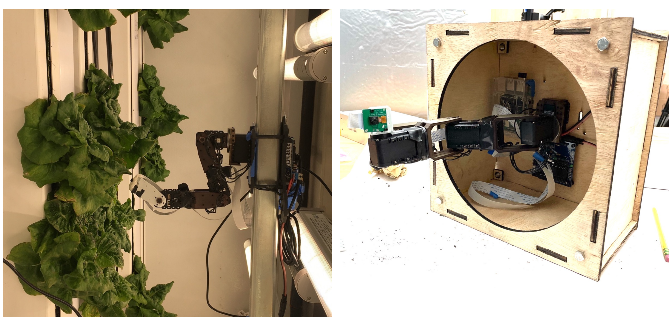

Fig. 3. 4DoF Robot arm with camera used to take a large number of photos from various angles of a single plant. Arm (without wooden cover and CDPR) taking photos of a plant (left). Arm inside wooden protective cover (right).

of photos of a plant from various, repeatable angles for use in structure from motion and other analysis techniques. Meanwhile, the CDPR enables analyzing a larger quantity of plants by moving the robot arm from plant to plant, enlarging the workspace of the robot arm to cover dozens of plants.

A. Mechanical Design

1) Robot Arm: The robot arm is dextrous to allow reaching around a plant to take a large number of photos from a variety of viewpoints. It is adapted from a Trossen Robotics PhantomX Pincher Mark II[1], which is a 4 degree of freedom (DoF) robot arm with a 31cm reach. The 3D CAD model, from which the kinematic geometry parameters can be ascertained, is available[2]. The robot arm was modified to replace the gripper with a Raspberry Pi Camera Module v2, which uses a IMX219 8MP sensor. The 4 DoF allow rotation in θ with the base joint and both translation and rotation in the $x-r$ plane (see Fig. 2). The completed robot arm is shown in Fig. 3.

2) CDPR: The CDPR is an 8-cable, 4-motor planar CDPR with a workspace of roughly 2.9m x 2.3m. Details on the CDPR design can be found in [36], with the primary distinctions being that (a) the robot arm shown in Fig. 3 is used in place of the spray paint carriage, and (b) the cables are doubled to provide more out-of-plane stability. The doubled cables consist of two cables spooled with two drums on a shared shaft driven by a single motor, as depicted in Fig. 4. The CDPR with robot arm are shown in Fig. 5

[1] https://web.archive.org/web/20190610001413/https://www.trossenrobotics.com/p/PhantomX-Pincher-Robot-Arm.aspx

[2] https://grabcad.com/library/interbotix-phantomx-pincher-robot-arm-kit-mark-ii-1

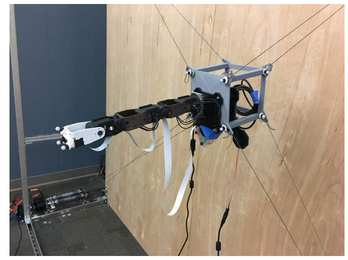

Fig. 4. Doubled, crossed cables provide additional out-of-plane stability.

Fig. 5. CDPR with robot arm. Dry-run without lettuce plants, without wooden protective cover for visual clarity, and arm mounted on the "outside" (left). Dry-run next to hydroponic grow rigs with wooden cover and arm mounted on the "inside" (right).

B. Electrical and Communication Design

A Raspberry Pi 4 controls the camera, robot arm, and CDPR using ROS, as overviewed in Fig. 6. The electronics are shown in Fig. 7, excepting the motor controllers and motors which are available in [36, Fig. 6 (right)].

The camera is connected directly to the Pi using a MIPI CSI-2 interface. During visual servo-ing, the camera is used in video mode to process 1080p frames at around 5fps. Upon completion of visual servo-ing, a final high-resolution (2592x1944) photo is taken and saved.

The robot arm is controlled through an Arbotix-M microcontroller which communicates to the Pi using rosserial over USB and to the servos using the DYNAMIXEL Protocol 1.0: a 1-wire, bidirectional, single-master-multiple-slave bus protocol. The robot arm inverse kinematics are implemented analytically and the task-space coordinates are defined in terms of θ, ϕ, x_c, r. The Pi issues servo position commands reads back positions to wait until successfully reaching the desired pose before proceeding.

The CDPR is controlled by a Teensy 4.1 which receives high-level cartesian position commands from the Pi and applies low-level motor torque commands to the motor controllers using the algorithm from Section III.A of [37].

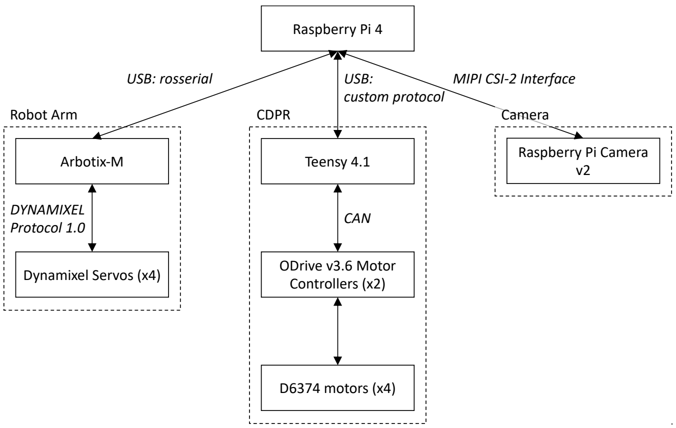

Fig. 6. System communication overview.

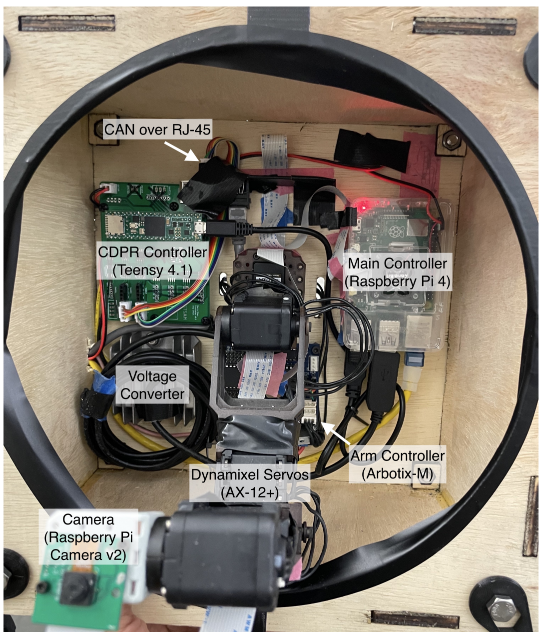

Fig. 7. Electronics mounted on the CDPR end-effector inside the protective wooden cover.

C. Data Collection Algorithm

The algorithm used for a data collection session, which consists of photographing all the plants, is summarized in Algorithm 2. Critical for collecting good quality photos is the visual-servo routine described in Algorithm 1, which is used to center the plants in the photos by panning up/down and zooming out as needed until the entire plant fits is contained in the photo.

IV. Evaluation Procedure

A. Dataset Collection Procedure

The data collection procedure is designed to collect photos, masses, and nutrient contents of approximately 48 total plants distributed across 6 different stages in their growth cycle.

The dataset collection procedure is as follows:

Algorithm 1 Visual Servo-ing to center the plant in a photo

Require: $\phi, \theta, x_{c,0}, r_0$
Ensure: photo
  $x_c, r \leftarrow x_{c,0}, r_0$
  move arm to (ϕ, θ, x_c, r)
  photo $\leftarrow$ `take_photo()`
  while !`is_centered(photo)` **do**
    $x, y, size \leftarrow$ `plant_center_and_size(photo)`
    translate up/down: $x_c \leftarrow \begin{cases} x_c + \delta_x & y < -\epsilon_y \\ x_c & -\epsilon_y \leq y \leq \epsilon_y \\ x_c - \delta_x & \epsilon_y < y \end{cases}$
    if $y > \epsilon_y$ or $y < -\epsilon_y$ or $size > size_{max}$ **then**
      zoom out: $r \leftarrow r + \delta_r$
    end if
    move arm to (ϕ, θ, x_c, r)
    photo $\leftarrow$ `take_photo()`
  end while
  return photo, (ϕ, θ, x_c, r)

Algorithm 2 Photographing of All Plants

  for plant index $i = 0$ to N **do**
    move CDPR to plant i
    for $\phi = \{\phi_0, \phi_1, \ldots, \phi_k\}$ **do**
      for $\theta = \{\theta_0, \theta_1, \ldots, \theta_k\}$ **do**
        photo $\leftarrow$ Algorithm 1: Visual Servo
        save [time, photo, (ϕ, θ, x_c, r)]
      end for
    end for
  end for

1) Start a new grow cycle for 8 plants each week for 6 weeks.
2) Upon transplanting the youngest set of 8 plants, photograph all the plants according to Algorithm 2, harvest all the plants, and measure the wet mass, dry mass, and nutrient contents (if applicable) of all plants.

Each grow cycle procedure is as follows:

1) Place 12 seeds (Bibb Butterhead Lettuce) in rockwool substrate.
2) Dampen the rockwool substate with water and place in an incubator next to grow lights for 14hrs/day, as shown in Fig. 8.
3) After 2 weeks, transplant up to 8 successfully germinated seedlings (randomly selected, if applicable) from the incubator to the vertical hydroponic growing towers. The grow tower conditions are under grow lights 14hrs/day; use *General Hydroponics Flora Series* fertilizer with ratios 3:2:1 of *FloraGro*, *FloraMicro*, and *FloraBloom* totalling 138ml of fertilizer per 100L of water; and are appropriately pH buffered according to the usage directions of *General Hydroponics pH Control Kit*.

The specifications for the grow lights, densities, and geometries are given in [], and the grow rig with cable robot is shown

Fig. 8. 1-week (left) and 0-week (right) old seedlings in the incubator (lid removed) prior to transplantation into the vertical grow towers at 2 weeks.

Fig. 9. The plant grow rig with cable robot, with the oldest plants being 28 days after transplant.

in Fig. 9.

The harvest and measurement procedure for each plant is as follows:

1) Cut the vegetative half of the plant as close to the grow medium/roots as is feasible.
2) Immediately measure the mass of the vegetative half of the plant on a scale to obtain the wet mass of the plant.
3) Dehydrate the plant for 48 hours.
4) Measure the mass of the dehydrated vegetative plant half to obtain the dry mass of the plant.
5) If there is sufficient quantity of sample, send the sample to an external lab for nutrient content testing.

To evaluate the quality of our dataset, we qualitatively compare the quality of the photos to 2 baseline methods: (1) top-down-only photos using an iPhone camera and (2) photos taken using the robot arm only with a human manually moving the arm to each new plant.

V. Results and Discussion

Our robot system is capable of autonomously collecting data at approximately 2640 photos per hour and spans 56 plants at a density of 54in^2/plant. Given the inherent scalability of cable robots, increasing the size of the cable robot to reach a greater number of plants is relatively straightforward while higher quality cameras can dramatically increase the photo capture rate by enabling faster shutter speeds or even continuous robot arm motion (currently, the arm must stop for each photo to eliminate motion blur and rolling shutter effects).

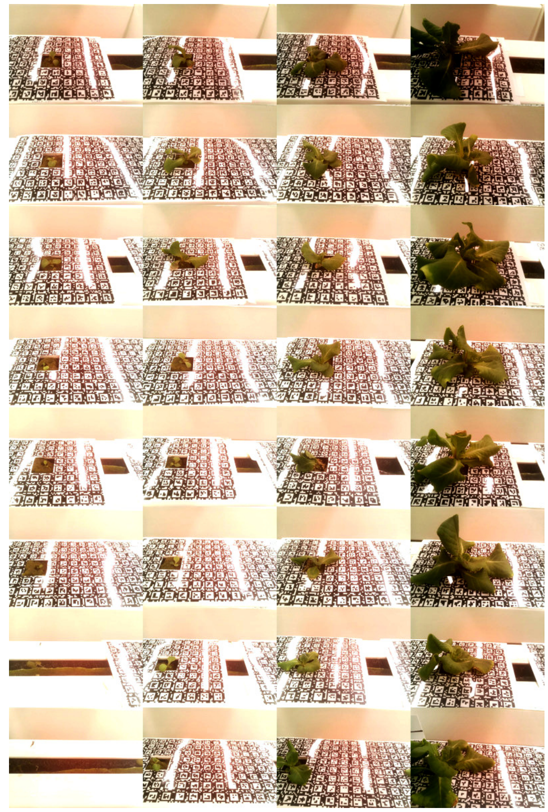

Fig. 10. Example photos from our plant dataset depicts 26 plants from the same relative camera angle.

TABLE I
Plant Age Distribution

Age (days since seed)	Age (days since transplant)	# of Samples
49	35	9
42	28	10
35	21	11
28	14	12
21	7	12
14	0	2

Using our robot system, we produce a dataset of 56 plants consisting of 150 photos of each plant as well as their ground truth wet masses, dry masses, and elemental nutrient contents. Fig. 10 depicts example photos from the dataset. The full dataset will be available online.

Our dataset evidences the efficacy and utility of our robot data collection platform. The speed and consistency with which photos are taken allows for higher throughput and quality data collection. We can compare the cable robot against 2 other baseline methods tested: (1) single top-down images and (2) an automated robot arm without cable robot.

Fig. 11 depicts the results from baseline 1: single top-down images. Although this has a low human labor requirement,

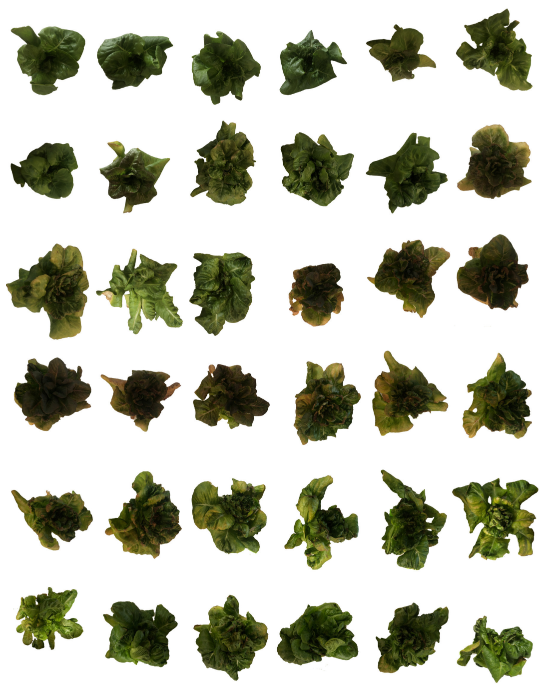

Fig. 11. Photos from baseline 1 of top-down photos from an iPhone camera (prior work by Andrew Sharkey). Only a single photo per plant was taken, limiting the comprehensiveness and predictive power of the data.

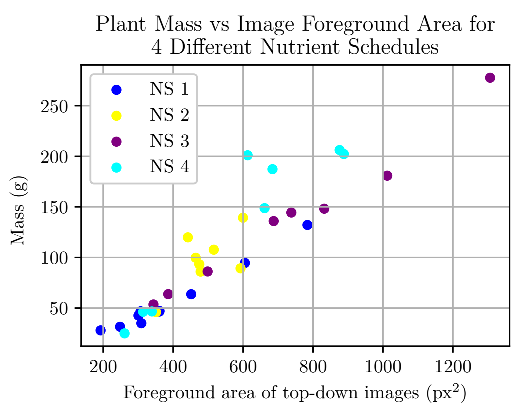

Fig. 12. Regression result using top-down photos from baseline 1 (prior work by Sushmita Warrier).

the maximum information that can be extracted from this data alone is limited. Prior work analyzing this dataset exhibits poor generalization to different nutrient schedules, with excess of 100% error for certain nutrient schedules, as shown in Fig. 12.

Fig. 13 depicts the results from baseline 2: photos taken by a robot arm but without the cable robot. Because the robot arm alone can only reach a single plant, a human is required to manually place the robot at each plant which not only increases human labor cost, but also introduces additional variability in the data due to imprecise robot placement. Both issues eliminate the possibility of this approach for high-throughput

Fig. 13. Photos from baseline 2 of photos takes using only the robot arm. Camera pose relative to the plant center is highly variable due to human placement error and human labor/oversight required is significant.

phenotyping in the current laboratory environment.

VI. Conclusions and Future Works

In conclusion, our robotic approach achieves our goals of higher-throughput data collection while also collecting photos from sufficient viewpoints so as to create 3D reconstructions of plants. As compared to baselines of (1) high-throughput but limited viewpoints/images per plant and (2) low-throughput but sufficient viewpoints/images per plant, our approach strikes a balance to autonomously collect large numbers of plant photos from a diverse, repeatable set of viewpoints.

The most immediate future work (within the next month) is to use the data to create plant mass and nutrient content estimates. Additional further works include testing with different nutrient schedules, using additional cameras (including depth, IR, and multi-/hyper- spectral), and increasing the scale of the cable robot to monitor a greater number of plants.

References

[1] EPA, "Inventory of u.s. greenhouse gas emissions and sinks: 1990-2020, chapter 5: Agriculture," U.S. Environmental Protection Agency 430-R-22-003, Tech. Rep., 2022.

[2] A. R. Cohen, G. Chen, E. M. Berger, S. Warrier, G. Lan, E. Grubert, F. Dellaert, and Y. Chen, "Dynamically controlled environment agriculture: Integrating machine learning and mechanistic and physiological models for sustainable food cultivation," *ACS ES&T Engineering*, vol. 2, no. 1, pp. 3–19, 2022. [Online]. Available: https://doi.org/10.1021/acsestengg.1c00269

[3] A. Paproki, X. Sirault, S. Berry, R. Furbank, and J. Fripp, "A novel mesh processing based technique for 3d plant analysis," *BMC Plant Biology*, vol. 12, 2012.

[4] J. Christian Rose, S. Paulus, and H. Kuhlmann, "Accuracy analysis of a multi-view stereo approach for phenotyping of tomato plants at the organ level," *Sensors (Switzerland)*, vol. 15, no. 5, pp. 9651–9665, 2015.

[5] J. Walter, J. Edwards, G. McDonald, and H. Kuchel, "Photogrammetry for the estimation of wheat biomass and harvest index," *Field Crops Research*, vol. 216, pp. 165–174, 2018.

[6] Z. Ni, T. F. Burks, and W. S. Lee, "3d reconstruction of plant/tree canopy using monocular and binocular vision," *Journal of Imaging*, vol. 2, no. 4, 2016. [Online]. Available: https://www.mdpi.com/2313-433X/2/4/28

[7] R. N. Lati, S. Filin, and H. Eizenberg, "Plant growth parameter estimation from sparse 3d reconstruction based on highly-textured feature points," *Precision Agriculture*, vol. 14, no. 6, pp. 586–605, 2013.

[8] J. Bendig, A. Bolten, S. Bennertz, J. Broscheit, S. Eichfuss, and G. Bareth, "Estimating biomass of barley using crop surface models (csms) derived from uav-based rgb imaging," *Remote Sensing*, vol. 6, no. 11, pp. 10 395–10 412, 2014.

[9] S. Brocks and G. Bareth, "Estimating barley biomass with crop surface models from oblique rgb imagery," *Remote Sensing*, vol. 10, no. 2, 2018.

[10] Y. Chéné, D. Rousseau, P. Lucidarme, J. Bertheloot, V. Caffier, P. Morel, É. Belin, and F. Chapeau-Blondeau, "On the use of depth camera for 3d phenotyping of entire plants," *Computers and Electronics in Agriculture*, vol. 82, pp. 122–127, 2012.

[11] G. Azzari, M. L. Goulden, and R. B. Rusu, "Rapid characterization of vegetation structure with a microsoft kinect sensor," *Sensors (Switzerland)*, vol. 13, no. 2, pp. 2384–2398, 2013.

[12] D. Andújar, C. Fernández-Quintanilla, and J. Dorado, "Matching the best viewing angle in depth cameras for biomass estimation based on poplar seedling geometry," *Sensors (Switzerland)*, vol. 15, no. 6, pp. 12 999–13 011, 2015.

[13] G. Alenyà, B. Dellen, and C. Torras, "3d modelling of leaves from color and tof data for robotized plant measuring," in *Proceedings - IEEE International Conference on Robotics and Automation*, 2011, pp. 3408–3414.

[14] G. Van Der Heijden, Y. Song, G. Horgan, G. Polder, A. Dieleman, M. Bink, A. Palloix, F. Van Eeuwijk, and C. Glasbey, "Spicy: towards automated phenotyping of large pepper plants in the greenhouse," *Funct. Plant Biol.*, vol. 39, no. 11, pp. 870–877, 2012.

[15] Y. Song, C. A. Glasbey, G. Polder, and G. W. A. M. van der Heijden, "Non-destructive automatic leaf area measurements by combining stereo and time-of-flight images," *IET Computer Vision*, vol. 8, no. 5, pp. 391–403, 2014.

[16] G. Polder and J. Hofstee, "Phenotyping large tomato plants in the greenhouse usig a 3d light-field camera," *American Society of Agricultural and Biological Engineers Annual International Meeting 2014, ASABE 2014*, vol. 1, pp. 153–159, 01 2014.

[17] T. T. Nguyen, D. C. Slaughter, N. Max, J. N. Maloof, and N. Sinha, "Structured light-based 3d reconstruction system for plants," *Sensors 2015, Vol. 15, Pages 18587-18612*, vol. 15, no. 8, pp. 18 587–18 612, 2015. [Online]. Available: https://www.mdpi.com/1424-8220/15/8/18587/htm

[18] M. R. Golzarian, R. A. Frick, K. Rajendran, B. Berger, S. Roy, M. Tester, and D. S. Lun, "Accurate inference of shoot biomass from high-throughput images of cereal plants," *Plant Methods*, vol. 7, no. 1, pp. 2–2, 2011.

[19] A. Hartmann, "Htpheno: an image analysis pipeline for high-throughput plant phenotyping," *BMC Bioinf.*, vol. 12, no. 148, pp. 1–9, 2011.

[20] T. Kataoka, T. Kaneko, H. Okamoto, and S. Hata, "Crop growth estimation system using machine vision," in *Proceedings 2003 IEEE/ASME International Conference on Advanced Intelligent Mechatronics (AIM 2003)*, vol. 2, 2003, pp. b1079–b1083 vol.2.

[21] G. E. Meyer, J. C. Neto, D. D. Jones, and T. W. Hindman, "Intensified fuzzy clusters for classifying plant, soil, and residue regions of interest from color images," *Computers and Electronics in Agriculture*, vol. 42, no. 3, pp. 161–180, 2004.

[22] G. E. Meyer and J. C. Neto, "Verification of color vegetation indices for automated crop imaging applications," *Computers and Electronics in Agriculture*, vol. 63, no. 2, pp. 282–293, 2008.

[23] L. Zheng, J. Zhang, and Q. Wang, "Mean-shift-based color segmentation of images containing green vegetation," *Computers and Electronics in Agriculture*, vol. 65, no. 1, pp. 93–98, 2009.

[24] K. J. Lee and B. W. Lee, "Estimation of rice growth and nitrogen nutrition status using color digital camera image analysis," *European Journal of Agronomy*, vol. 48, pp. 57–65, 2013.

[25] M. Guijarro, G. Pajares, I. Riomoros, P. J. Herrera, X. P. Burgos-Artizzu, and A. Ribeiro, "Automatic segmentation of relevant textures in agricultural images," *Computers and Electronics in Agriculture*, vol. 75, no. 1, pp. 75–83, 2011.

[26] L. Zheng, D. Shi, and J. Zhang, "Segmentation of green vegetation of crop canopy images based on mean shift and fisher linear discriminant," *Pattern Recognition Letters*, vol. 31, no. 9, pp. 920–925, 2010.

[27] W. z. Liang, K. R. Kirk, and J. K. Greene, "Estimation of soybean leaf area, edge, and defoliation using color image analysis," *Computers and Electronics in Agriculture*, vol. 150, pp. 41–51, 2018.

[28] S. Aich, A. Josuttes, I. Ovsyannikov, K. Strueby, I. Ahmed, H. S. Duddu, C. Pozniak, S. Shirtliffe, and I. Stavness, "Deepwheat: Estimating phenotypic traits from crop images with deep learning," in *2018 IEEE Winter Conference on Applications of Computer Vision (WACV)*, 2018, pp. 323–332.

[29] B. T. Kitano, C. C. T. Mendes, A. R. Geus, H. C. Oliveira, and J. R. Souza, "Corn plant counting using deep learning and uav images," *IEEE Geoscience and Remote Sensing Letters*, pp. 1–5, 2019.

[30] J. M. Chen and J. Cihlar, "Quantifying the effect of canopy architecture on optical measurements of leaf area index using two gap size analysis methods," *IEEE Transactions on Geoscience and Remote Sensing*, vol. 33, no. 3, pp. 777–787, 1995.

[31] Y. Zhang, J. M. Chen, and J. R. Miller, "Determining digital hemispherical photograph exposure for leaf area index estimation," *Agricultural and Forest Meteorology*, vol. 133, no. 1-4, pp. 166–181, 2005.

[32] K. Kirk, H. J. Andersen, A. G. Thomsen, J. R. Jørgensen, and R. N. Jørgensen, "Estimation of leaf area index in cereal crops using red-green images," *Biosystems Engineering*, vol. 104, no. 3, pp. 308–317, 2009.

[33] S. Tang, J. M. Chen, Q. Zhu, X. Li, M. Chen, R. Sun, Y. Zhou, F. Deng, and D. Xie, "Lai inversion algorithm based on directional reflectance kernels," *Journal of Environmental Management*, vol. 85, no. 3, pp. 638–648, 2007.

[34] S. Garrigues, N. V. Shabanov, K. Swanson, J. T. Morisette, F. Baret, and R. B. Myneni, "Intercomparison and sensitivity analysis of leaf area index retrievals from lai-2000, accupar, and digital hemispherical photography over croplands," *Agricultural and Forest Meteorology*, vol. 148, no. 8-9, pp. 1193–1209, 2008.

[35] J. Casadesus and D. Villegas, "Simple digital photography for assessing biomass and leaf area index in cereals," *BIO-PROTOCOL*, vol. 5, 2015.

[36] G. Chen, S. Baek, J.-D. Florez, W. Qian, S. won Leigh, S. Hutchinson, and F. Dellaert, "Extended version of GTGraffiti: Spray painting graffiti art from human painting motions with a cable driven parallel robot," 2021.

[37] G. Chen, S. Hutchinson, and F. Dellaert, "Locally optimal estimation and control of cable driven parallel robots using time varying linear quadratic gaussian (LQG) control," https://gerry-chen.com/publications/Chen22iros_cdpr_control/Chen22iros_cdpr_tracking_control.pdf, 2022.